Surface enhanced sum frequency generation of carbon monoxide adsorbed on platinum nanoparticle arrays

Steve Baldelli and Aaron S. Eppler
Department of Chemistry, University of California at Berkeley, Berkeley, California 94720 and Materials Science Division, Lawrence Berkeley National Laboratory, Berkeley, California

Erik Anderson
Materials Science Division, Lawrence Berkeley National Laboratory, Berkeley, California

Yuen-Ron Shen
Materials Science Division, Lawrence Berkeley National Laboratory, Berkeley, California and Department of Physics, University of California at Berkeley, Berkeley, California 94720

Gabor A. Somorjai
Department of Chemistry, University of California at Berkeley, Berkeley, California 94720 and Materials Science Division, Lawrence Berkeley National Laboratory, Berkeley, California

(Received 22 May 2000; accepted 6 July 2000)

Sum frequency generation (SFG) vibrational spectroscopy is used to study the adsorption of CO at ~1 atm pressure on Pt nanoparticle arrays and Pt thin films. The SFG signal of CO adsorbed on platinum particles of 45 nm diameter is ~10 000 times larger than from CO on smooth Pt films. The large enhancement is explained by plasmon resonance and Maxwell–Garnett theory. The Pt arrays are prepared using electron beam lithography to produce particles with uniform spacing and sizes on an oxidized Si(100) wafer. Further, as the Pt coverage increases the SFG signal shows a polarization dependence that is explained considering the dielectric properties of a metal film on a dielectric surface. In addition, SFG permits investigation of the CO adsorbed on the particles at ~1 atm, which is not possible with most surface analytical techniques, that will allow for the study of the reaction of small molecules on surfaces relevant in heterogeneous catalysis. © *2000 American Institute of Physics.* [S0021-9606(00)70437-5]

INTRODUCTION

Many of the molecular details of catalytic reactions have been determined by using vibrational spectroscopy to probe transition metal single crystal model surfaces.[1] Yet, industrial catalysis is mostly carried out on metal nanoparticles deposited on high surface area oxides (SiO_2, TiO_2, Al_2O_3, etc.) In order to understand the behavior of these real catalysts on a molecular level, electron beam lithography is used to fabricate a model system that permits systematic variation of the size, composition, and interparticle spacing of transition metal nanoparticles. A microscopic understanding of the reaction mechanisms in heterogeneous catalysis is a major goal in surface chemistry.

In this article sum frequency generation (SFG) vibrational spectroscopy is used to study the adsorption of CO on Pt nanoparticle arrays. The SFG signal of CO adsorbed to the Pt particles exhibits an enhancement of 10 000× compared to CO adsorbed on a smooth Pt film. Although the SFG signal originates from CO on the metal particles, the polarization dependence of the SFG signal indicates the optical properties are dominated by the oxidized Si(100) substrate. Despite the low surface area (<5% of a monolayer) of these nanoparticle arrays, surface spectroscopy can be performed due to the large electromagnetic enhancements at the surface of small metal particles.

BACKGROUND

The SFG experimental procedure has been described previously.[2] Sum frequency generation is achieved by spatially and temporally overlapping a 532 nm and infrared beam at the sample surface. As the infrared frequency is scanned, and corresponds to a vibrational resonance of an adsorbed molecule, there is an increase in the sum frequency intensity. A plot of the infrared frequency vs. SFG intensity is interpreted as a vibrational spectrum of the surface molecules. Sum frequency generation is a second order, $\chi^{(2)}$, process and in the electric dipole approximation, occurs only in environments without inversion symmetry, such as an interface between two isotropic media.

$$I_{\mathrm{SF}} \propto \left| \sum \chi^{(2)}_{IJK} \mathbf{E}_{\mathrm{VIS}} \mathbf{E}_{\mathrm{IR}} \right|^2. \tag{1}$$

The SFG intensity ($\mathbf{I}_{\mathrm{SF}}$) is proportional to the square of the nonlinear susceptibility ($\chi^{(2)}_{\mathrm{IJK}}$) in surface reference frame IJK and the electric fields at the surface, **E**.
The surface susceptibility $\chi^{(2)}$ is composed of a resonant and nonresonant part

$$\chi^{(2)} = \chi^{(2)}_R + \chi^{(2)}_{\mathrm{NR}} = \chi^{(2)}_{\mathrm{NR}} + \sum_q \frac{A_q}{\omega_{\mathrm{IR}} - \omega_q + i\Gamma}. \tag{2}$$

The A_q term contains the Raman and infrared line strengths for the qth vibrational mode at frequency ω_q with a damping

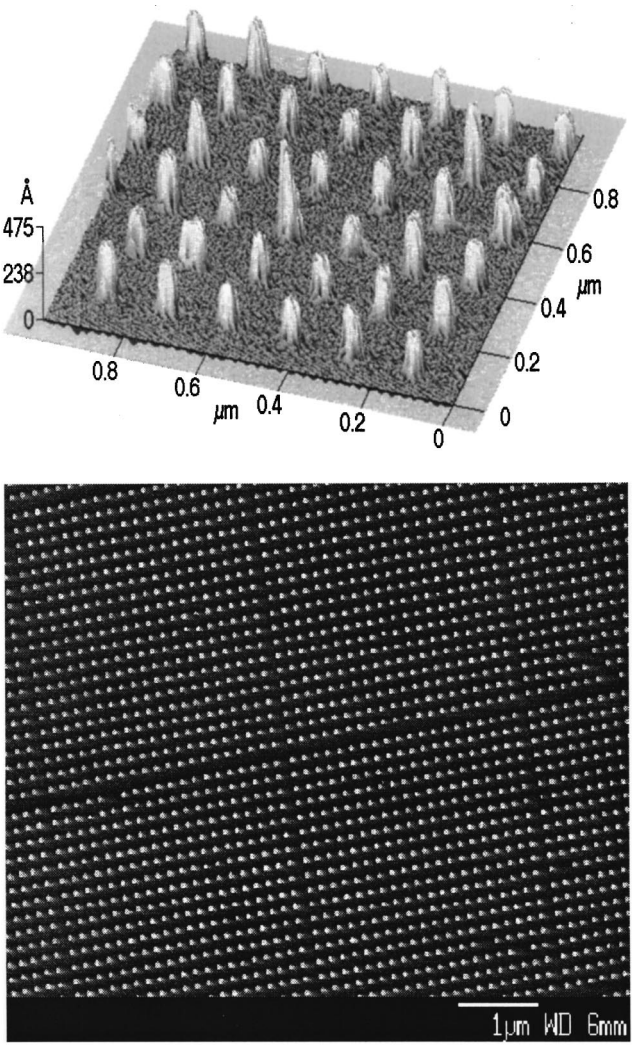

FIG. 1. AFM and SEM micrograph of platinum nanoparticle array. Particles are 40 nm diameter spaced 150 nm between particles.

constant of Γ, ω_{IR} is the frequency of the infrared beam. Equation (2) is used to curve fit the spectra and extract information on the mode strength and peak position.

EXPERIMENT

The generation of the picosecond midinfrared light pulses is accomplished in two stages by optical parametric generation/amplification of 532 nm light in β-barium borate crystals followed by difference frequency mixing of the near infrared idler beam with 1064 nm light in a $AgGaS_2$ crystal.[3] The 532 nm and infrared beam diameters are ~2 mm and ~1 mm with energy densities of 6 mJ/cm^2 and 3 mJ/cm^2, respectively. This energy density is below the damage threshold of the nanoparticle arrays as shown by the scanning electron micrograph in Fig. 1. The 532 nm and infrared beams define the $x-z$ plane and are at an angle of incidence of 50° and 60°, respectively. The samples are aligned with the rows parallel to the plane of incidence of the laser beams, although sample rotation has no effect on the SFG signal.

To ensure data are easily comparable, all spectra are referenced to the SFG intensity of the oxidized silicon surface with *ssp* polarization. The spectra shown in Fig. 2 are the average of three spectra each with 50 shots/point divided by the infrared and 532 nm beam intensity at each point. Error bars represent one standard deviation.

The nanoparticle arrays are fabricated using electron beam lithography (EBL). The first step in the EBL fabrication process is to spin-coat polymethyl methacrylate (PMMA) (MW=950 000) onto a Si(100) wafer with 5 nm thick SiO_2 on the surface. Computer-designed patterns are then ''written'' into the polymer layer with a highly collimated electron beam (Leica column) generated by a field emission source. With a beam current of 600 pA and accelerating voltage of 100 kV, the beam diameter is approximately 8 nm. A dose of 2500 mC/cm^2 (4×10^{-16} C/site) was used to expose the PMMA, resulting in a dwell time of about 0.6 ms at each particle site. Following dissolution of the exposed polymer, a 15 nm thick film of Pt is then deposited on the sample by electron beam evaporation. Finally, the remaining resist is removed (''lifted off'') by dissolution with organic solvent and the metal particles of the prescribed pattern remained on the substrate. With this high degree of spatial resolution, 36 mm^2 arrays with approximately 10^9 metal particles were produced.

Samples are cleaned by dipping into freshly prepared 50/50 V/V of concentrated HNO_3/H_2SO_4 solution for 3–4 min, rinsed with triple distilled water, and dried in a stream of nitrogen gas. The particles are then immediately placed into a Teflon® cell with ~1 atm CO (Scott Specialty gas). CO is purified by flowing through a molecular sieve column before entering the SFG cell. The same procedure is used for both the platinum particles and metal films. The samples are placed in the same cell at the same time for a direct comparison between nanoparticles and the metal film.

RESULTS

Sum frequency generation spectra of CO on Pt films and nanoparticles are taken with various polarization combinations of incoming and outgoing beams, *s* or *p* polarized. The SFG spectra of three samples are shown in Fig. 2. Figure 2(a) are the SFG spectra of CO on 45 nm platinum nanoparticles spaced 150 nm apart. The CO peak is at 2085 cm^{-1}, shifted by -15 cm^{-1} from clean polycrystalline platinum; this peak is assigned to CO coordinated to one platinum atom and the wavelength shift is likely due to coadsorbed water from the cleaning procedure.[4] The intensity ratio for the 45 nm particles is 26:2:1 for *ssp* (*s*-sum frequency, *s*-visible, *p*-infrared), *ppp*, and *sps* polarization combinations, respectively. Figure 2(b) are SFG spectra for nanoparticles with 200 nm diameters and spaced 100 nm apart. One peak is seen at 2085 cm^{-1}.

The intensity ratio between the *ssp*, *ppp*, and *sps* spectra is ~5:35:1. Figure 2(c) are the spectra of CO on the platinum film with *ssp*, *ppp*, and *sps* polarization combinations. The peak at ~2085 cm^{-1} is due to CO coordinated to one platinum atom, top site CO.[5] The intensity of the *ppp* spectrum of the metal film is ~5 times more intense than *ssp* with very little resonant signal for *sps* polarization 1:4:$<$0.5 for *ssp*, *ppp*, and *sps*, respectively. All other polarization combinations have no resonant features in the SFG spectrum. There are also no peaks between 1800–2150 cm^{-1} in the SFG

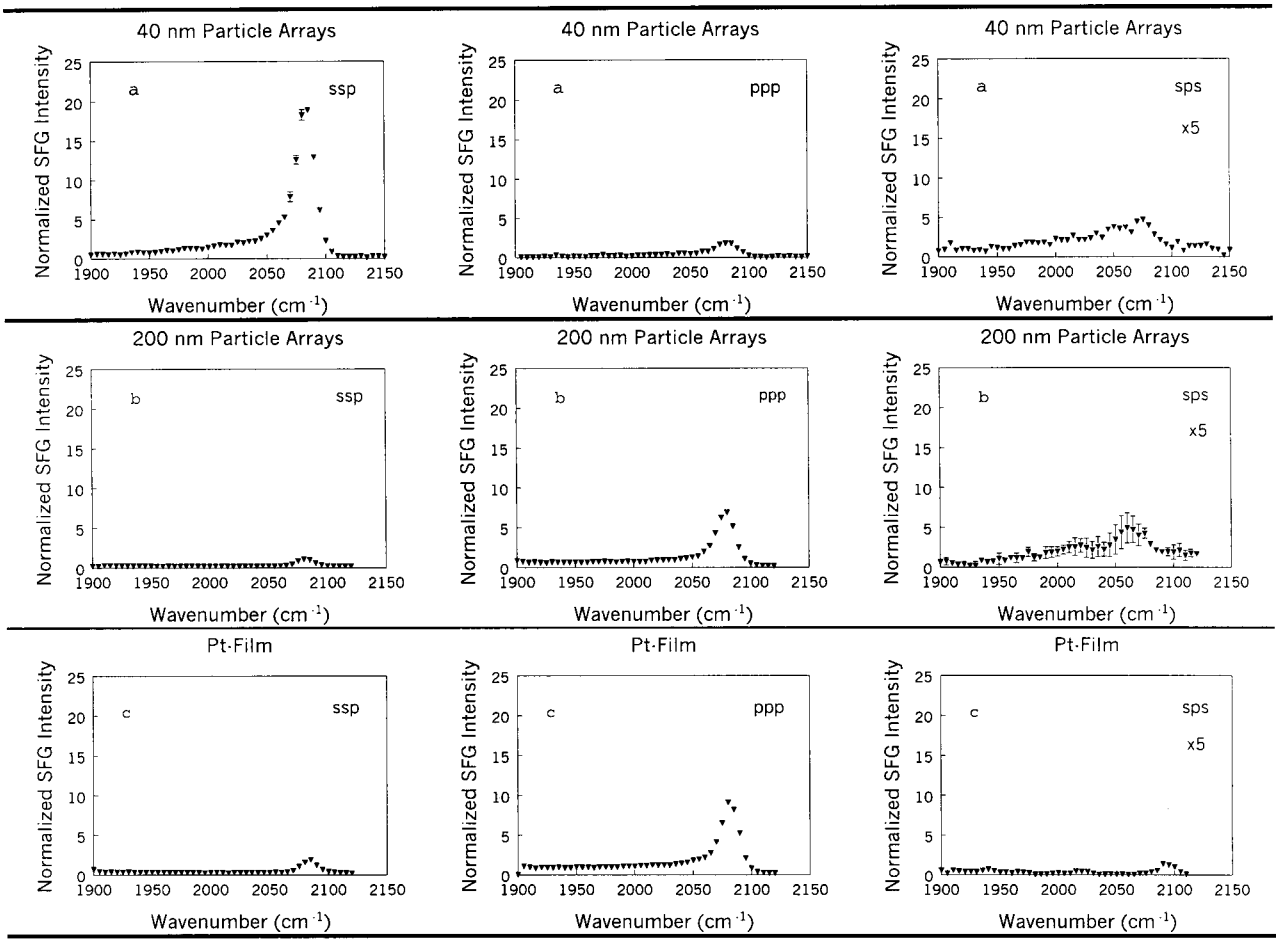

FIG. 2. SFG spectra of CO adsorbed on (a) 40 nm Pt nanoparticle arrays, (b) 200 nm Pt nanoparticle arrays, (c) smooth Pt film. For each sample, the three spectra are shown: *ssp*, *ppp* and *sps* polarization.

spectrum of the silicon surface under 1 atm. CO indicating CO does not orient on the oxidized silicon surface. A summary of the data is presented in Table I.

To compare the signal, in *ssp* polarization, from the particles sample to the Pt film the results of the signal from the particles divided by the signal of the smooth film accounting for the surface coverage of CO and laser beam intensities, $G=(I_{SF}^{(\text{particle})}/\theta_{\text{particle}}^2)/(I_{\text{SF}}^{(\text{film})}/\theta_{\text{film}}^2)$, are shown in Fig. 3. Sum frequency generation intensity ratio above 1 indicates enhancement compared to the smooth platinum surface. The surface coverage of CO, θ_{CO}, is assumed proportional to the coverage of Pt on the oxidized silicon substrate in each sample. These parameters are shown in Table I. The maximum enhancement for these particles is ~10 000 for particles of ~45 nm diameter with *ssp* polarization.

DISCUSSION

For several years researchers have noted the enhancement of optical fields at small silver particles or rough silver surfaces. These effects are observed in Raman,[6–9] hyper-Raman,[10] two-photon absorption,[11] second harmonic generation (SHG),[6,12] and four-wave mixing,[13] Most experiments have been devoted to understanding the phenomenon

TABLE I. Summary of particle data.

Sample particle dia. (nm)	Surface coverage (θ)	$I_{\text{SF}}(ssp)$ (a.u.)	$I_{\text{SF}}(ppp)$ (a.u.)	$I_{\text{SF}}(sps)$ (a.u.)	G_{ssp}	G_{ppp}	G_{sps}
6	0.5	59	5	3	141	7	24
30	0.065	86	12	15	1696	66	3550
40	0.043	94	14	⋯	4236	176	⋯
45	0.054	412	31	16	11774	247	5486
200	0.45	5	8	12	40	48	59
1000	0.58	2	9	>0.5	3	15	1
Smooth Pt film	1.0	12	43	>0.5	1	1	1

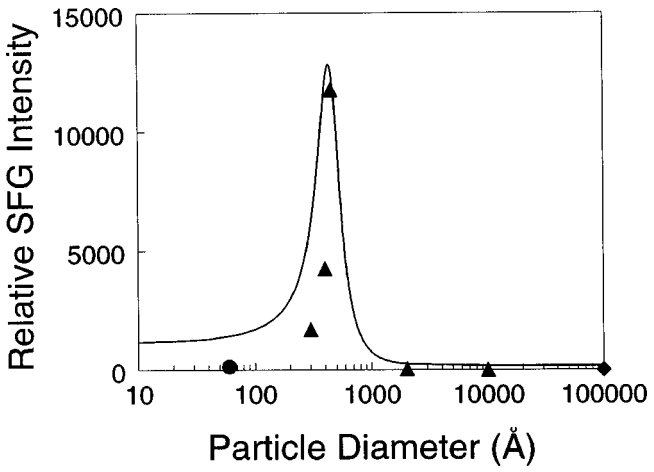

FIG. 3. SFG Intensity vs particle diameter. ▲-nanoparticle arrays fabricate with *e*-beam lithography. ●-Pt clusters deposited by evaporation. ♦-Pt metal film. Solid line is predicted intensity based on plasmon resonance and substrate contributions to the local fields.

of surface enhanced Raman scattering (SERS). These reports focus on arguments that an electromagnetic mechanism is more important than a chemical mechanism for the increased signal. The electromagnetic enhancement mechanism states, briefly, that when electromagnetic waves interact with a metal particle that is smaller than the wavelength of incident light, surface plasmon are excited which results in increased electromagnetic field intensities at the surface. The increased surface intensity thus leads to larger surface signals in, for example, Raman spectroscopy. According to the chemical enhancement mechanism, increase in signal intensity is due primarily to the adsorbed molecule forming a type of surface complex with the metal. This new surface complex then contains new electronic energy levels with which electromagnetic waves may be resonant.[14,15] Many researchers now believe both effects contribute to the observed enhancement, and which is dominant probably depends on the system under investigation.[6,8,16,17] For the SFG experiment considered here, the electromagnetic enhancement mechanism is favored, since an electromagnetic model accounts for the observed intensity of the SFG signal.

To explain the SFG intensities on the nanoparticles, the particle size, shape, material, particle spacing, and substrate must be considered. The size, shape, and material effects are based on the idea that surface plasmons are excited on small metal particles, which enhance the local fields of the laser beam. The particle spacing affects the coupling between particles as well as any diffraction effects of the array. Finally, the dielectric properties of the substrate influence the macroscopic fields at the surface that is determined by the metal coverage and this is accounted for with a modified Maxwell–Garnett equation.

The enhancement at small metal particles is governed by particle size and shape and based on the Mie resonance criteria.[12,18,19] The shape of the particle dramatically affects the Mie resonance condition. As the particle becomes more ellipsoidal, the Mie resonance shifts to lower energies closer to the visible region of the spectrum. Therefore based on shape the more needle-like particles have a larger enhancement. This is also known as the lightning rod effect. Further enhancement is due to small particle size. Qualitatively, this is due to a polarization of the conduction electrons that contributes to the electric field at the surface.

To account for the local electromagnetic field intensities at the surface, $\mathbf{E}_{\mathrm{loc}}$, a local field correction factor, f is used:

$$\mathbf{E}_{\mathrm{loc}} = f \cdot \mathbf{E}_0,$$

where $\mathbf{E}_0$ is the incident field. The correction factor is composed of two terms,

$$f = (E_f)(E_{\mathrm{PR}}),$$

where E_f is the Fresnel factor calculated for a three layer system of Si/nanoparticle/air.[20,21] This is the substrate effect on the local fields and is discussed below.[21]

The local field enhancement due to plasmon resonance, E_{PR}, is determined by

$$E_{\mathrm{PR}}^2 = \frac{|\epsilon|^2}{\{1-[1-\mathrm{Re}(\epsilon)]A_{\mathrm{eff}}+\mathrm{Im}(\epsilon)(4\pi^2 V/3\lambda^3)\}^2+\{\mathrm{Im}(\epsilon)A_{\mathrm{eff}}+[1-\mathrm{Re}(\epsilon)](4\pi^2 V/3\lambda^3)\}^2}. \quad (3)$$

A_{eff} is the depolarization factor that depends on the particle shape and is 0.5 for cylindrical particles.[19,22] The term $(4\pi^2 V/3\lambda^3)$ of Eq. (3) is due to the radiation damping of the particle resonance where V is the particle volume and λ is the wavelength of light. This term accounts for decrease in the enhancement, as the particles become large.[23] Local field enhancement also decreases for very small particles, <25 nm, due to surface scattering effects, where the mean free path of the conduction electrons is less than the particle dimensions and is accounted for with the size dependant dielectric constant of Pt, ϵ.[24,25] The size dependant ϵ is only significantly different from the bulk dielectric constant for particles <25 nm.[25] A plot of $E_{\mathrm{PR}}^{2\mathrm{total}}$ vs. particle diameter is shown in Fig. 4(a). The contribution to the enhancement from to the sum frequency and visible light fields is ~ 2 times greater than that from the infrared field, respectively, since the SF and visible fields are closer to the plasmon resonance frequency. The total field enhancement of the particles due to plasmon resonance is $E_{\mathrm{PR}}^{2\mathrm{total}} = (E_{\mathrm{PR}}^{2\mathrm{SF}} E_{\mathrm{PR}}^{2\mathrm{Vis}} E_{\mathrm{PR}}^{2\mathrm{IR}}) \approx 175$ for ~ 50 nm particles.

To determine the local fields due to depositing metal particles on a dielectric substrate Fresnel's equations for a three-layer system are used. To calculate the dielectric constant of the interfacial region, Maxwell–Garnett theory is

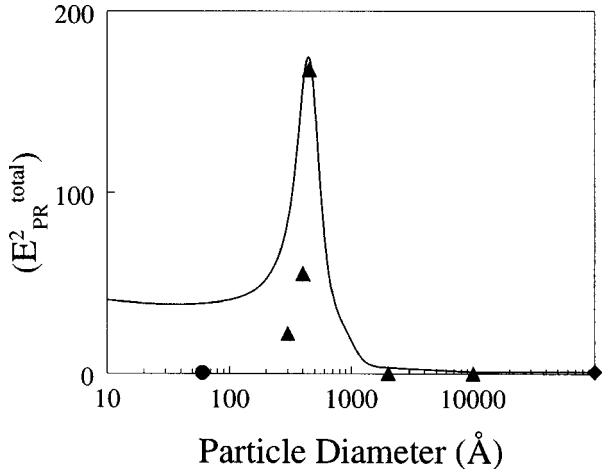

FIG. 4. Enhancement of SFG signal from CO adsorbed on Pt nanoparticles as a function of particle size. (a) ▼-nanoparticle arrays fabricate with *e*-beam lithography. ●-Pt clusters deposited by evaporation. ♦-Pt metal film. Line is predicted total enhancement due to plasmon resonance from Eq. (3).

used. For the nanoparticles deposited on oxidized Si the surface fields are determined by both the dielectric properties of the SiO_2 and the metal in a nonlinear way. This will affect the absolute SFG signal as well as the relative intensities of the different polarization combinations. The polarization spectra in Fig. 2 show that the highest intensity is for the *ssp* polarization for particles and *ppp* polarization for the metal film. This result may at first seem surprising since the CO signal originates locally only from the metal surface in both cases and therefore the polarization spectra should look the same. This result is explained using Maxwell–Garnett theory for metal particles on a dielectric surface.[26–28] A plot of the real and imaginary portion of the effective refractive index, n_e, for the surface is shown in Fig. 5. These plots are generated from the following equations:[28]

$$n_e^2=\frac{1+2rq}{1-rq} \quad \text{where} \quad r=\frac{n^2-1}{n^2+1}. \tag{4}$$

The q in this equation is the packing density of the particles on the surfaces where q is between 0 and 1 for no metal and a full monolayer, respectively, n is the bulk refractive index of the metal. Most of the nanoparticle samples used here have a packing density <0.25. This indicates the surface is effectively an insulator since the metallic properties become noticeable for packing density $q>\sim 0.5$ [Fig. 2(b)]. For the 200 nm particles $q\sim 0.6$, k, the imaginary portion of the dielectric constant, becomes larger and the surface is more metallic which causes the CO signal in the *ppp* spectrum to be more intense than in *ssp*. Using the dielectric values determined from Eq. (4) in Fresnel's equation for a three layer system leads to the larger surface fields for the SFG signal in *ssp* over *ppp* polarization for low coverage nanoparticle samples. For example the enhancement of the light fields due to the substrate for the particles compared to the metal film for *ssp* polarization is

$$E^2_{f,ssp}=\frac{\text{particles}}{\text{metal film}}=\frac{(E_f^y)^2(E_f^y)^2(E_f^z)^2}{(E_f^y)^2(E_f^y)^2(E_f^z)^2}=76,$$

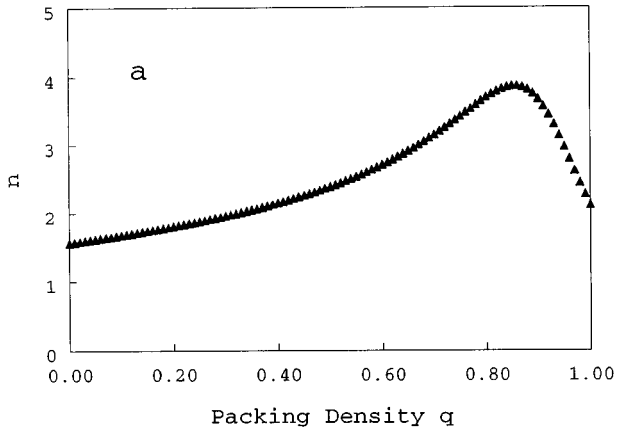

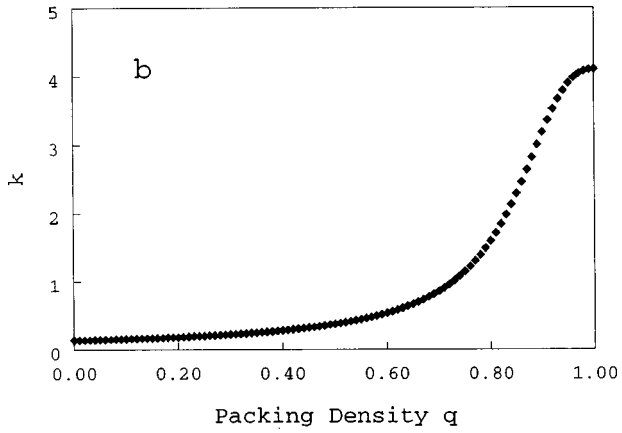

FIG. 5. (a) Real (n) and (b) imaginary (k) portion of the dielectric constant for the nanoparticle surface as a function of q, the packing density. Bulk refractive index for platinum $1.96+3.42i$ at 532 nm (Ref. 24).

for the 45 nm diameter particle sample.

The calculated SFG intensity enhancement here is about 10^4 for particles $\approx$50 nm diameter. About 30% of this enhancement is due to the substrate effect and 70% is due to plasmon resonance in small metal particles. Table II shows the substrate effect and plasmon resonance on the SFG signal from particles compared to the smooth metal film for *ssp* polarization. This calculation provides an order-of-magnitude explanation of the surface enhancement. A more quantitative estimate can be achieved using the discrete dipole approximation of Schatz and Van Duyne.[29]

TABLE II. Calculated enhancement factors for platinum nanoparticles.

Particle diameter (nm)	Plasmon resonance Factor $(E^2_{PR})^{total}$	Substrate factor $(E^2_{f,ssp})$	Total $(f)^2$
6	28	76	2128
30	76	76	5776
40	160	76	12 160
45	178	70	12 460
200	1	60	60
1000	1	64	60
Smooth metal	1	1	1

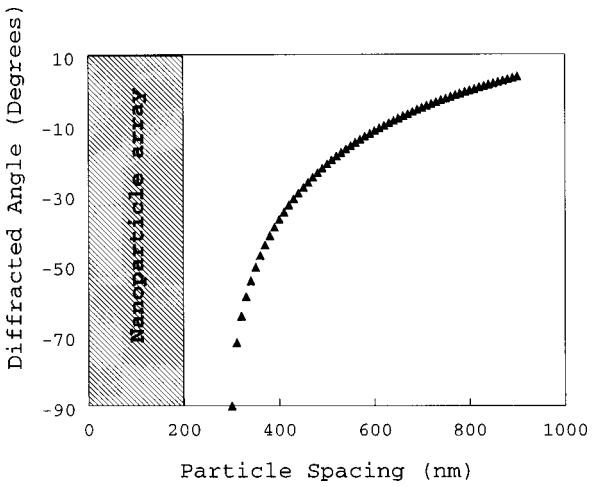

FIG. 6. Calculated diffracted SFG signal as function of particle spacing. All particle arrays have spacing below 200 nm, in the zeroth-order diffraction region, that is below 300 nm.

The CO signal is an average over the entire particle since the wavelength is much longer than the particle dimensions. The results of Eq. (3) predict enhancement over the entire particle since it is the electrons in the metal that are polarized. The signal is averaged over the entire particle and thus signal from the side or top of the particle cannot be separated. The maximum enhancement occurs at sharp points on the particle where the fields have the highest intensity; this is the lightning rod effect.[7,30] Therefore, the polarization spectra are not probing different orientations of CO but the polarization dependence is only determined by the effective dielectric constant of the surface as discussed above. Orientation information is lost on nanoparticles, i.e., the polarization information no longer relates to the orientation of the CO on the nanoparticle, whereas on the smooth Pt film the CO molecular coordinates can be related to the experimental geometry.[31] Instead the difference in the polarization spectra is due to the changing dielectric properties of the surface as the metal coverage increases. This is clear in Fig. 5 where the imaginary portion of the dielectric, k, increases, as the substrate becomes more metallic at higher packing ratio of Pt clusters. Similarly, the intensity ratio in the ssp/ppp spectra also decrease since s-polarized fields are decreased relative to the incident beam while p-polarized fields are increased for a metal surface.[20,32]

Since the particles are in a regular two-dimensional array, dispersion effects might be expected. There is no diffraction for particle spacing less 310 nm. Therefore, this experiment is not effected by the periodic array, i.e., grating effect. This experiment is in the zeroth-order diffraction (Fig. 6).[18]

CONCLUSION

Sum frequency generation provides a method for studying model nanoparticle catalysts. Without surface enhancement, the vibrational spectra of adsorbates would be unattainable on such systems. Since the surface coverage of these particles is already $<5\%$ of a monolayer this approaches the detection limits for typical vibrational spectroscopies such as infrared absorption and high resolution electron loss spectroscopy.[1] The local coverage of CO on the platinum particles is near saturation, ~ 0.5 monolayer. Further, these spectra are obtained at pressure ~ 1 atm of CO that is only possible with a surface sensitive technique such as SFG.

Most reports of surface enhanced effects are reported on silver, copper, or gold surfaces.[16] The enhancement observed here on platinum is not typical. The reason why this modest enhancement is seen here and not previously in SERS experiments is probably due to the coherent nature of the SFG signal which allows for more efficient collection of the signal compared to the scattering of Raman signal. Also since the particles have very low size dispersion all the particles will contribute to the signal since they are all in the Mie resonance.

SFG signal is enhanced at small platinum particles due to the interaction of the light with the surface plasmons. The enhanced signal allows for the study of catalytic reactions on model nanoparticle surfaces under reaction conditions.

ACKNOWLEDGMENTS

This work is supported by the Director, Office of Energy Research, Office of Basic Energy Sciences, Material Science Division of the U.S. Department of Energy under Contract No. DeAC03-76F00098 and No. DeAC03-7600099.

[1] G. A. Somorjai, *Introduction to Surface Chemistry and Catalysis*, 1st ed. (Wiley, New York, 1994).
[2] S. Baldelli, N. Markovic, P. N. Ross, Y. R. Shen, and G. A. Somorjai, J. Phys. Chem. B **103**, 8920 (1999).
[3] J. Y. Zhang, J. Y. Huang, and Y. R. Shen, *Optical Parametric Generation and Amplification*, 1st ed. (Harwood Academic, Luxembourg, 1995).
[4] S. Chang, L. H. Leung, and M. J. Weaver, J. Phys. Chem. **93**, 5341 (1989).
[5] N. Sheppard and T. T. Nguyen, in *Advances in Infrared and Raman Spectroscopy*, edited by R. J. H. Clark and R. E. Hester (Heyden and Sons, Philadelphia, 1978), Vol. 5, p. 67.
[6] C. K. Chen, T. F. Heinz, D. Ricard, and Y. R. Shen, Phys. Rev. B **27**, 1965 (1983).
[7] J. I. Gersten, J. Chem. Phys. **72**, 5779 (1980).
[8] D. L. Mills and M. Weber, Phys. Rev. B **26**, 1075 (1982).
[9] S. Nie and S. R. Emory, Science **275**, 1102 (1997).
[10] J. T. Golab, J. R. Spague, K. T. Carron, G. C. Schatz, and R. P. V. Duyne, J. Chem. Phys. **88**, 7942 (1988).
[11] P. C. Das, H. Metiu, and A. Puri, J. Chem. Phys. **89**, 6497 (1988).
[12] G. Berkovic and S. Efrima, Langmuir **9**, 355 (1993).
[13] D. S. Chemla, J. P. Heritage, P. F. Liao, and E. D. Isaacs, Phys. Rev. B **27**, 4553 (1983).
[14] V. M. Hallmark and A. Campion, J. Chem. Phys. **84**, 2933 (1986).
[15] P. Kambhampati, C. M. Child, M. C. Foster, and A. Campion, J. Chem. Phys. **108**, 5013 (1998).
[16] B. Pettinger, in *Adsorption of Molecules at Metal Electrodes*, edited by J. Lipkowski and P. N. Ross (VCH, New York, 1992), Vol. 1, pp. 414.
[17] M. Moskovits, Rev. Mod. Phys. **57**, 783 (1985).
[18] A. Wokaun, J. G. Bergman, J. P. Heritage, A. M. Glass, P. F. Liao, and D. H. Olson, Phys. Rev. B **24**, 849 (1981).
[19] P. F. Liao and M. B. Stern, Opt. Lett. **7**, 483 (1982).
[20] A. Campion, Annu. Rev. Phys. Chem. **36**, 549 (1985).
[21] M. B. Feller, W. Chen, and Y. R. Shen, Phys. Rev. A **43**, 6778 (1991).
[22] J. A. Osborn, Phys. Rev. **67**, 351 (1945).
[23] A. Wokaun, J. P. Gordon, and P. F. Liao, Phys. Rev. Lett. **48**, 957 (1982).
[24] *Handbook of Chemistry and Physics*, edited by D. R. Lide (CRC, Boca Raton, 1992).
[25] U. Kreibig and C. V. Fragstein, Z. Phys. **224**, 307 (1969).

[26] J. G. Bergman, D. S. Chemla, P. F. Liao, A. M. Glass, A. Pinczuk, R. M. Hart, and D. H. Olson, Opt. Lett. **6**, 33 (1981).
[27] T. Yamaguchi, S. Yoshida, and A. Kinbara, Thin Solid Films **18**, 63 (1973).
[28] O. S. Heavens, *Optical Properties of Thin Solid Films* (Dover, New York, 1991).
[29] W. H. Yang, G. C. Schatz, and R. P. V. Duyne, J. Chem. Phys. **103**, 869 (1995).
[30] P. F. Liao and A. Wokaun, J. Chem. Phys. **76**, 751 (1982).
[31] C. Hirose, N. Akamatsu, and K. Domen, J. Chem. Phys. **96**, 997 (1992).
[32] R. G. Greenler, J. Chem. Phys. **50**, 1963 (1969).